主論文

The renin–angiotensin system promotes arrhythmogenic substrates and lethal arrhythmias in mice with non-ischaemic cardiomyopathy

Chinatsu Yamada[1], Koichiro Kuwahara[1]*, Masatoshi Yamazaki[2], Yasuaki Nakagawa[1], Toshio Nishikimi[1], Hideyuki Kinoshita[1], Yoshihiro Kuwabara[1], Takeya Minami[1], Yuko Yamada[1,3], Junko Shibata[1], Kazuhiro Nakao[1,3], Kosai Cho[1], Yuji Arai[4], Haruo Honjo[2], Kaichiro Kamiya[2], Kazuwa Nakao[5], and Takeshi Kimura[1]

[1]Department of Cardiovascular Medicine, Kyoto University Graduate School of Medicine, 54 Shogoin Kawaharacho, Sakyo-ku, Kyoto 606-8507, Japan; [2]Research Institute of Environmental Medicine, Nagoya University, Nagoya, Japan; [3]Department of Peptide Research, Kyoto University Graduate School of Medicine, Kyoto, Japan; [4]Department of Bioscience and Genetics, National Cerebral and Cardiovascular Center Research Institute, Suita, Japan; and [5]Medical Innovation Center, Kyoto University Graduate School of Medicine, Kyoto, Japan

Aims	The progression of pathological left ventricular remodelling leads to cardiac dysfunction and contributes to the occurrence of malignant arrhythmias and sudden cardiac death. The underlying molecular mechanisms remain unclear, however. Our aim was to examine the role of the renin–angiotensin system (RAS) in the mechanism underlying arrhythmogenic cardiac remodelling using a transgenic mouse expressing a cardiac-specific dominant-negative form of neuron-restrictive silencer factor (dnNRSF-Tg). This mouse model exhibits progressive cardiac dysfunction leading to lethal arrhythmias.
Methods and results	Subcutaneous administration of aliskiren, a direct renin inhibitor, significantly suppressed the progression of pathological cardiac remodelling and improved survival among dnNRSF-Tg mice while reducing arrhythmogenicity. Genetic deletion of the angiotensin type 1a receptor (AT1aR) similarly suppressed cardiac remodelling and sudden death. In optical mapping analyses, spontaneous ventricular tachycardia (VT) and fibrillation (VF) initiated by breakthrough-type excitations originating from focal activation sites and maintained by functional re-entry were observed in dnNRSF-Tg hearts. Under constant pacing, dnNRSF-Tg hearts exhibited markedly slowed conduction velocity, which likely contributes to the arrhythmogenic substrate. Aliskiren treatment increased conduction velocity and reduced the incidence of sustained VT. These effects were associated with suppression of cardiac fibrosis and restoration of connexin 43 expression in dnNRSF-Tg ventricles.
Conclusion	Renin inhibition or genetic deletion of AT1aR suppresses pathological cardiac remodelling that leads to the generation of substrates maintaining VT/VF and reduces the occurrence of sudden death in dnNRSF-Tg mice. These findings demonstrate the significant contribution of RAS activation to the progression of arrhythmogenic substrates.
Keywords	Renin–angiotensin system • Sudden • Cardiac • Arrhythmia • Electrical remodelling

1. Introduction

Ventricular tachyarrhythmia is a major cause of morbidity and mortality in patients with heart failure. Sudden cardiac death, generally preceded by the development of ventricular tachycardia (VT) or fibrillation (VF), accounts for ~50% of deaths among heart failure patients.[1] Although it appears that multiple mechanisms, including abnormal impulse initiation (the trigger) and a pre-existing arrhythmogenic substrate for initiation and maintenance of re-entry, are coordinately involved in the development of lethal arrhythmias, the precise molecular mechanisms mediating the initiation and maintenance of VT and VF in failing hearts remain largely undefined.[2,3]

We previously reported that a transcriptional repressor, neuron-restrictive silencer factor (NRSF, also named REST), is an important regulator of the fetal cardiac gene programme, and generated transgenic mice cardiac-specifically expressing a dominant-negative mutant of

---

* Corresponding author. Tel: +81 75 751 4287; fax: +81 75 771 9452, E-mail: kuwa@kuhp.kyoto-u.ac.jp

NRSF (dnNRSF-Tg).[4] These dnNRSF-Tg mice exhibit progressive cardiomyopathy and sudden arrhythmic death, beginning at ∼8 weeks of age.[4] In addition, dnNRSF-Tg hearts exhibit increased expression of fetal cardiac genes commonly observed in hypertrophied and failing hearts in both rodents and humans, suggesting that this mouse model is a representative and useful model of non-ischaemic cardiomyopathy accompanied by lethal arrhythmias. In our earlier studies, we demonstrated that blockade of fetal type cardiac ion channels [T-type Ca^{2+} channels (TCC) or hyperpolarization-activated cyclic nucleotide-gated (HCN) channels] reduced the incidence of sudden death among dnNRSF-Tg mice.[5,6] However, this approach did not prevent the pathological remodelling observed in dnNRSF-Tg ventricles, which suggests that these channels are involved largely in the generation of the trigger for the arrhythmias, not the substrate.

The renin−angiotensin system (RAS) is a pivotal signalling pathway often involved in the development of cardiovascular diseases. Indeed, activation of RAS is associated with an increased risk for ventricular tachyarrhythmias;[3] however, the effect of RAS signalling on the occurrence of lethal arrhythmias and their underlying mechanisms is less certain. In this study, we used optical mapping analysis of cardiac action potentials to assess the role of RAS activation in the mechanism underlying the remodelling that leads to generation of arrhythmogenic substrates in dnNRSF-Tg mice. We found that both pharmacological blockade of RAS activation using a direct renin inhibitor and genetic deletion of the angiotensin II type 1a receptor (AT1aR) significantly ameliorated pathological cardiac remodelling and suppressed the generation of arrhythmogenic substrates and sudden cardiac death in dnNRSF-Tg mice. These beneficial effects were achieved, at least in part, through attenuation of cardiac fibrosis and restoration of expression of connexin 43 (Cx43). Our findings provide direct evidence that the RAS contributes critically to the progression of arrhythmogenic remodelling that leads to generation of arrhythmogenic substrates in non-ischaemic cardiomyopathy accompanied by lethal arrhythmias.

2. Methods

An expanded Methods section is available in Supplementary material online.

2.1 Animal experiments

The animal care and all experimental protocols were reviewed and approved by the Animal Research Committee at the Kyoto University Graduate School of Medicine, and conformed to the US National Institute of Health Guide for the Care and Use of Laboratory Animals. Beginning at 16 weeks of age, male dnNRSF-Tg or wild-type (WT) mice were treated for 12 weeks with aliskiren (23 mg/kg/day s.c.) or vehicle (untreated) using osmotic minipumps (ALZET osmotic pumps, DURECT Corporation, Cupertino, CA, USA) according to the manufacture's protocol. The doses of the drugs were chosen based on earlier reports and our preliminary studies.[7] Aliskiren was provided by Novartis Pharma AG (Basel, Switzerland). In another experiment, male dnNRSF-Tg and WT mice were treated for 6 weeks with aliskiren at the same dose (23 mg/kg/day s.c.), beginning when they were 12 weeks of age.

To obtain dnNRSF-Tg;AT1aR$^{-/-}$ mice and their control dnNRSF-Tg;AT1aR$^{+/+}$ littermates, dnNRSF-Tg mice (C57BL/6 background) were bred with AT1aR knockout mice (C57BL/6 background). AT1aR$^{-/-}$ mice were described in an earlier report.[8]

For the isolation and analysis of hearts, mice were anaesthetized with 3.0% of isoflurane and sacrificed by cervical dislocation. For the implantation of osmotic minipumps and radiofrequency transmitters, mice were anaesthetized with sodium pentobarbital injected intraperitoneally (40 mg/kg).

2.2 Measurement of plasma hormone concentrations

Plasma renin activity and aldosterone concentrations were measured using a Gamma Coat Plasma Renin Activity kit (Dade Behring, Tokyo, Japan) and an SPAC-S aldosterone kit (Daiichi Radioisotope Laboratories, Tokyo, Japan).

2.3 Measurement of haemodynamics and cardiac function

Blood pressure, echocardiography, and haemodynamic parameters were measured as previously described.[4]

2.4 Histological analysis

Consecutive tissue sections from hearts fixed in 10% formalin were stained with haematoxylin and eosin (HE) and with Masson's trichrome using standard staining techniques. Immunohistochemical analysis was performed using an anti-Cx43 antibody (1 : 100 dilution, #3512, Cell Signaling Technology).

2.5 Quantitative PCR and western blot analysis

Relative mRNA levels were determined using quantitative real-time PCR, as previously described.[6] Western blot analysis was carried out using lysates from mouse ventricles, as described previously.[6]

2.6 Intracardiac electrophysiology

Intracardiac electrophysiological studies were performed on mice intubated and anaesthetized, as described previously.[4]

2.7 Optical mapping

The procedures for optical mapping were essentially the same as described previously.[9] Briefly, hearts were perfused on a Langendorff apparatus with modified Krebs-Ringer solution at 37°C. The tissue was then loaded with a voltage-sensitive dye, di-4-ANEPPS (4 μM, 10 min), and fluorescence images (256 × 256 pixels) were recorded at 1000 frames/s using a solid-state image-sensing digital video camera (Fastcam-Max, Photron, Japan). The data obtained were analysed using the software written in our laboratory.[9]

2.8 Statistical analysis

Survival was analysed using the Kaplan−Meier method with the log-rank test. Unpaired t-tests were used for comparisons between two independent groups, whereas paired t-tests were used for comparisons between two groups that were correlated. One-way ANOVA with post hoc Fisher's tests was used for comparisons among three groups, and two-way ANOVA with post hoc Fisher's tests was used for comparison among four groups containing two variables. Numbers of premature ventricular contractions (PVCs) and episodes of VT were compared between two groups using the non-parametric Mann−Whitney test. The incidences of VT among dnNRSF-Tg mice during the intracardiac electrophysiological and optical mapping studies were analysed using Fisher's exact test. Values of $P < 0.05$ were considered significant.

3. Results

## 3.1 Direct renin inhibition improves survival among dnNRSF-Tg mice

Plasma renin activity, aldosterone concentrations, and angiotensin II concentrations were all significantly higher in dnNSRF-Tg mice than in WT littermates (*Figure 1A* and *B*, and see Supplementary material online, *Figure S1A*). To determine the role played by RAS in the progression of cardiomyopathy and sudden arrhythmic death in dnNRSF-Tg mice, we subcutaneously administered aliskiren, a direct renin inhibitor, for 12 weeks at 23 mg/kg/day, beginning when the
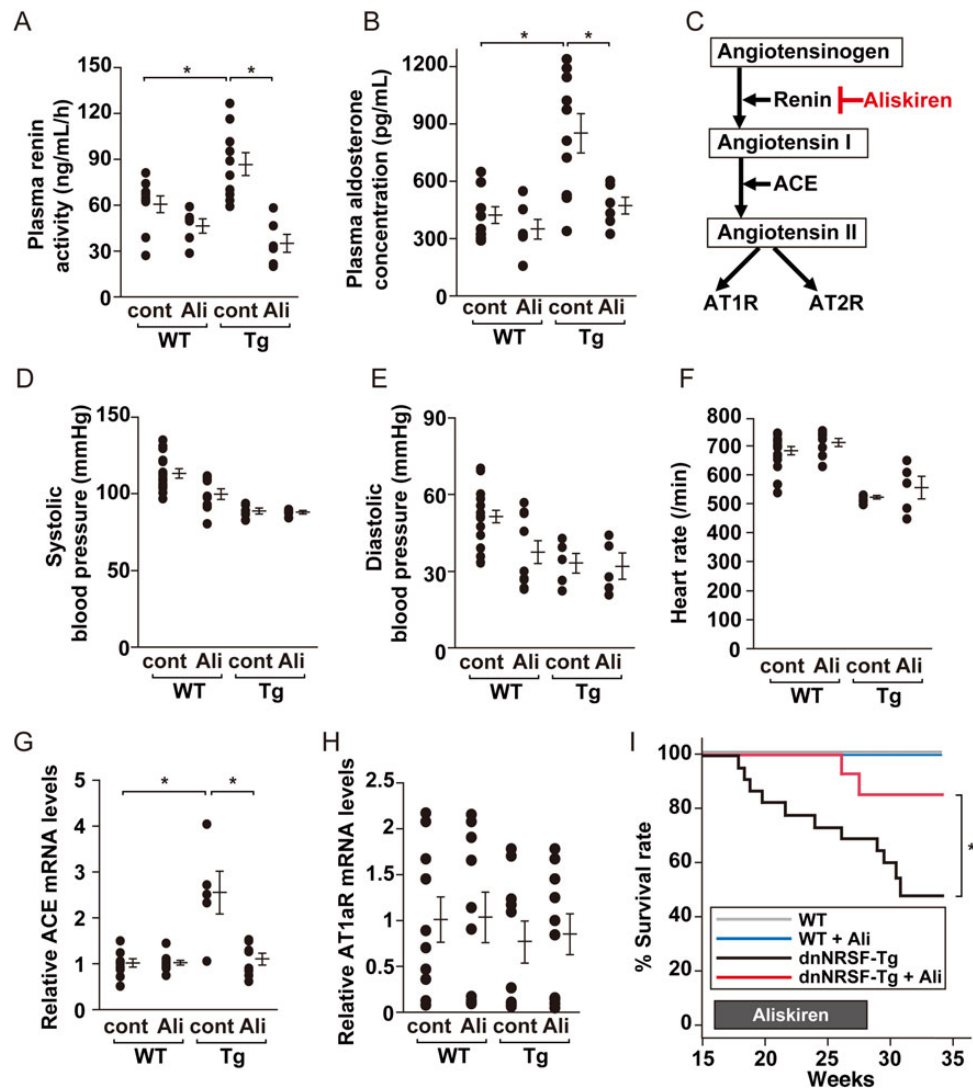
Figure 1 Renin inhibition prolongs survival among dnNRSF-Tg (Tg) mice. (*A* and *B*) Plasma renin activity (*A*) and aldosterone concentrations (*B*) in 28-week-old WT and dnNRSF-Tg mice, with or without aliskiren (Ali; *n* = 9 for untreated WT, 6 for aliskiren-treated WT, 10 for untreated Tg, and 6 for aliskiren-treated Tg mice). (*C*) Diagram illustrating the RAS and the action of aliskiren on that system. AT1R: angiotensin type 1 receptor; AT2R: angiotensin type 2 receptor; ACE: angiotensin-converting enzyme. (*D*−*F*) Systolic blood pressure (*D*), diastolic blood pressure (*E*), and heart rates (*F*) in 28-week-old WT and dnNRSF-Tg mice, with and without aliskiren (Ali) (*n* = 16 for untreated control WT, 9 for WT with aliskiren, and 5 for untreated control Tg and Tg with aliskiren). (*G* and *H*) Gene expression of cardiac ACE (*G*) and AT1aR (*H*) in WT and dnNRSF-Tg, with or without aliskiren (*n* = 10 for untreated and aliskiren-treated WT, 5 for untreated Tg, and 8 for aliskiren-treated Tg mice). All data are shown as dot plots and means ± SEM. *$P < 0.05$. (*I*) Kaplan−Meier survival curves for dnNRSF-Tg, with or without aliskiren. Aliskiren treatment began when the mice were 16 weeks of age and lasted 12 weeks: *$P < 0.05$ (*n* = 54 for untreated Tg, 28 for aliskiren-treated Tg, and 10 for untreated and aliskiren-treated WT mice).

mice were 16 weeks of age (*Figure 1C*). The dose of aliskiren did not affect blood pressure in dnNRSF-Tg mice, which had significantly lower systolic blood pressures than in WT mice (*Figure 1D* and *E*). Heart rates were significantly slower in dnNRSF-Tg than in WT mice, but aliskiren did not affect heart rates (*Figure 1F*). As expected, aliskiren significantly reduced plasma renin activity and angiotensin II concentrations (*Figure 1A* and see Supplementary material online, *Figure S1A*) and markedly suppressed the increase in plasma aldosterone levels otherwise seen in dnNRSF-Tg mice (*Figure 1B*). This indicates that sufficient systemic RAS inhibition was achieved with aliskiren at the dose used. In addition, to evaluate local RAS activity, we also measured ventricular expression of several mRNAs encoding RAS-related proteins,

including renin, angiotensin-converting enzyme (ACE), angiotensinogen, AT1aR, and (pro) renin receptor, and measured cardiac angiotensin II concentrations. Among these, expression of ACE mRNA was significantly increased in the ventricles of untreated dnNRSF-Tg mice, but this enhancement was reversed by aliskiren (*Figure 1G*). Ventricular angiotensin II concentrations were higher in untreated dnNRSF-Tg mice, and aliskiren also significantly suppressed that increase (see Supplementary material online, *Figure S1B*). Expression of AT1aR mRNA and protein levels did not significantly differ among the four groups (*Figure 1H* and see Supplementary material online, *Figure S1C*), nor did expression of renin, angiotensinogen, or (pro) renin receptor mRNA (see Supplementary material online, *Figure S1D−F*).
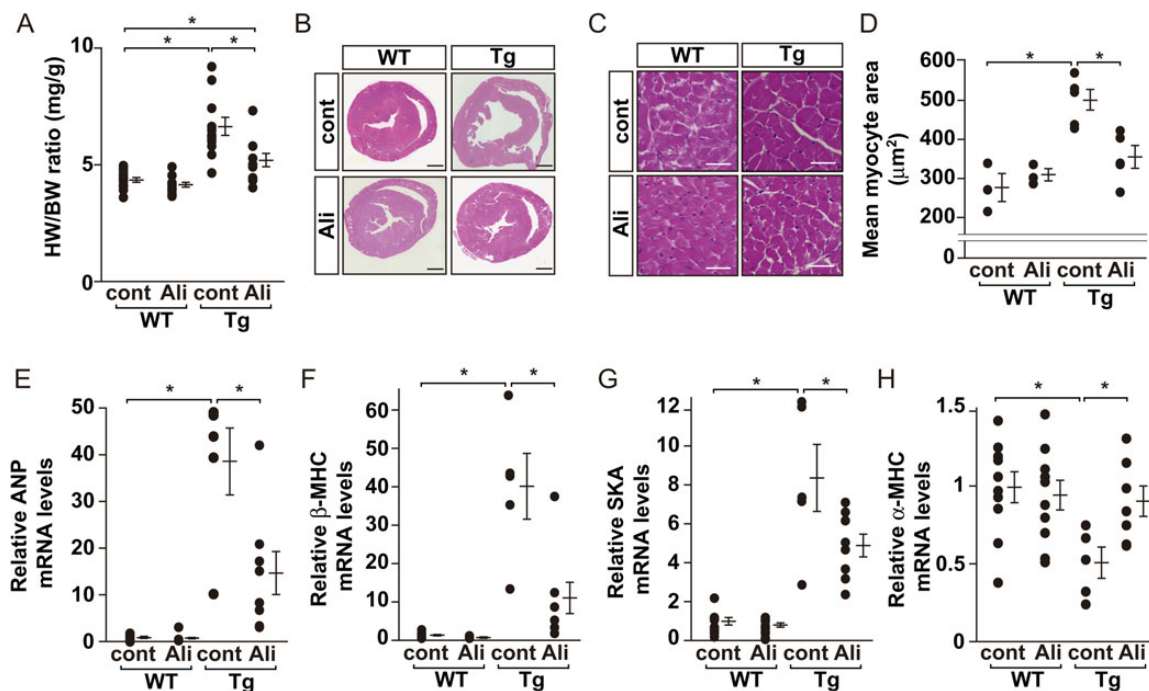
Figure 2 Effects of renin inhibition on cardiac remodelling in dnNRSF-Tg mice. (A) Heart weight-to-body weight ratios (HW/BW) in 28-week-old WT and Tg, with or without aliskiren (Ali; $n = 16$ for untreated WT, 12 for aliskiren-treated WT, 11 for untreated Tg, and 10 for aliskiren-treated Tg mice). (B−D) Histological analysis of hearts from 28-week-old WT and dnNRSF-Tg, with or without aliskiren: HE, haematoxylin−eosin staining. (B) HE-stained coronal sections of hearts. Scale bars, 1 mm. (C) Photomicrographs of HE-stained LV sections. Scale bars, 40 μm. (D) Areas of individual myocardial cells in left ventricles. Bars are mean myocyte areas measured in 100 cells in each group ($n = 3$ for untreated WT and WT with aliskiren and 5 for untreated Tg and Tg with aliskiren). (E−H) Relative levels of ANP (E), β-MHC (F), skeletal α-actin (G), and α-MHC (H) mRNA in hearts from 28-week-old WT and dnNRSF-Tg, with or without aliskiren (Ali; $n = 10$ for untreated and aliskiren-treated WT, 5 for untreated Tg, and 8 for aliskiren-treated Tg mice). Unless indicated otherwise, aliskiren treatment began when the mice were 16 weeks of age and lasted 12 weeks. All data are shown as dot plots and means $\pm$ SEM. *$P < 0.05$.

Collectively, the effects of aliskiren in dnNRSF-Tg mice significantly improved survival (*Figure 1I*).

3.2 Renin inhibition prevents the progression of pathological ventricular remodelling in dnNRSF-Tg mice

We next examined the effects of aliskiren on cardiac structure and function. Heart-to-body weight ratios in untreated dnNRSF-Tg mice, which are higher than in WT mice,[4,5] were significantly reduced by aliskiren (*Figure 2A*). Body weights were not significantly affected by aliskiren, irrespective of genotype (see Supplementary material online, *Figure S2A*). Echocardiographic analysis performed with conscious mice showed that the ejection fraction was significantly lower and the left ventricular (LV) diastolic and systolic diameters were both increased in 28-week-old untreated dnNRSF-Tg mice, when compared with age-matched WT mice, which is consistent with earlier findings (*Table 1* and see Supplementary material online, *Figure S2B*).[5,10] Aliskiren prevented the deterioration of these echocardiographic parameters during the treatment period (*Table 1* and see Supplementary material online, *Figure S2C−E*).

Haemodynamic measurements performed on 22-week-old mice after left cardiac catheterization showed that LV end-diastolic pressure was significantly higher and +dP/dt was significantly lower in untreated dnNRSF-Tg than WT hearts, as described previously (*Table 1* and see

Supplementary material online, *Figure S3A and B*).[4] −dP/dt was also significantly depressed in untreated dnNRSF-Tg (*Table 1* and see Supplementary material online, *Figure S3B*), and aliskiren significantly improved all these haemodynamic parameters (*Table 1* and see Supplementary material online, *Figure S3A and B*).

To evaluate aliskiren's ability to prevent pathological cardiac remodelling in younger dnNRSF-Tg mice, we also treated 12-week-old mice with aliskiren for 6 weeks (from 12 to 18 weeks of age). Examination following the treatment showed that aliskiren partially, but significantly, prevented the increase in heart-to-body weight ratios and deterioration in cardiac function in dnNRSF-Tg mice (see Supplementary material online, *Figure S4A−E*).

Histological analysis of ventricular cross-sections revealed LV dilatation and thinning of the ventricular wall in untreated dnNRSF-Tg hearts, which were both prevented by aliskiren (*Figure 2B*). Mean myocyte size was significantly greater in untreated dnNRSF-Tg than in WT hearts, but aliskiren significantly reduced myocyte size in dnNSRF-Tg hearts (*Figure 2C and D*).

The results summarized above suggest that aliskiren prevents pathological cardiac remodelling in dnNRSF-Tg mice. To further confirm that idea, we evaluated the expression of fetal cardiac genes as sensitive markers for pathological remodelling. When we measured the gene expression of atrial natriuretic peptide (ANP), β-myosin heavy chain (MHC), and skeletal α-actin mRNA in ventricles from 28-week-old

Table 1 Echocardiographic and haemodynamic parameters in WT and dnNRSF-Tg mice, with or without aliskiren treatment

	WT		dnNRSF-Tg	
	Untreated	**Ali**	**Untreated**	**Ali**
Echocardiographic data				
Heart rate (/min)	719 ± 9.7	711 ± 12.6	586 ± 12.1	588 ± 16.7
LVDd (mm)	2.8 ± 0.14	2.7 ± 0.12	4.2 ± 0.27	3.7 ± 0.12
LVDs (mm)	1.1 ± 0.098	1.2 ± 0.067	3.6 ± 0.29	2.9 ± 0.17
IVST (mm)	0.62 ± 0.03	0.63 ± 0.04	0.52 ± 0.04	0.57 ± 0.03
PWT (mm)	0.65 ± 0.04	0.65 ± 0.03	0.50 ± 0.03	0.48 ± 0.02
EF (%)	93.0 ± 1.1	91.5 ± 0.8	36.0 ± 4.2*	52.9 ± 4.4*†
FS (%)	59.7 ± 2.3	56.2 ± 1.5	14.2 ± 2.2*	22.8 ± 2.4*†
Haemodynamic data				
LVSP (mmHg)	89.1 ± 8.2	83.0 ± 3.8	81.9 ± 8.4	82.5 ± 4.2
LVEDP (mmHg)	3.2 ± 0.6	2.3 ± 0.4	8.6 ± 2.1*	2.2 ± 1.3†
dP/dt (mmHg/s)	9189 ± 347	8871 ± 753	3922 ± 898*	7091 ± 766†
−dP/dt (mmHg/s)	−5789 ± 421	−6418 ± 569	−2966 ± 585*	−6375 ± 704†

Values are means ± SEM. Echocardiographic parameters were measured in 28-week-old WT and dnNRSF-Tg mice, with or without 12 weeks of aliskiren treatment. Haemodynamic parameters were measured in 22-week-old WT and dnNRSF-Tg mice, with or without 6 weeks of aliskiren treatment. Numbers of mice tested in echocardiographic analyses were 11 for untreated control WT and 10 for WT with aliskiren, untreated dnNRSF-Tg and dnNRSF-Tg with aliskiren. Numbers of mice catheterized were three for untreated control WT and untreated dnNRSF-Tg and four for WT with aliskiren and dnNRSF-Tg with aliskiren.
Ali, mice treated with aliskiren; LVDd, left ventricular diastolic dimension; LVDs, left ventricular systolic dimension; IVST, interventricular septum thickness; PWT, posterior wall thickness; EF, ejection fraction; FS, fractional shortening; LVSP, left ventricular systolic pressure; LVEDP, left ventricular end-diastolic pressure; dP/dt, first derivative of pressure.
*P < 0.05 vs. untreated WT mice.
†P < 0.05 vs. untreated dnNRSF-Tg mice.

mice, we found their expression levels to be significantly higher in untreated dnNRSF-Tg than in WT mice (*Figure 2E–G*). Moreover, the increase in the expression of these genes in dnNRSF-Tg mice was significantly suppressed by aliskiren (*Figure 2E–G*). Conversely, transcription of the α-MHC and sarco(endo)plasmic reticulum Ca^{2+}-ATPase isoform 2 (SERCA2) genes was reduced in untreated dnNRSF-Tg mice, but was significantly restored by treatment with aliskiren (*Figure 2H* and see Supplementary material online, *Figure S5A*). Finally, expression of *CACNA1H*, encoding the TCC α1 subunit, and *HCN2* and *4*, all of which are directly regulated by NRSF, was higher in dnNRSF-Tg than in WT mice, but the expression levels did not significantly differ between untreated mice and those treated with aliskiren (see Supplementary material online, *Figure S5B–D*).[4]

3.3 Renin inhibition suppresses malignant arrhythmias in dnNRSF-Tg mice

We next used a telemetric monitoring system to examine the effects of aliskiren on the incidence of arrhythmias. As previously described, dnNRSF-Tg mice exhibited frequent PVCs and VTs, both of which were suppressed by aliskiren (*Figure 3A* and *B*). We previously showed that at a similar age, WT mice showed no such arrhythmias.[5] Because aliskiren ameliorated the progression of pathological cardiac remodelling without affecting NRSF-regulated fetal cardiac ion channel gene expression, we hypothesized that the drug primarily suppressed the generation of arrhythmogenic re-entrant substrates in dnNRSF-Tg hearts. To test that idea, we carried out an *in vivo* intracardiac electrophysiological analysis in dnNRSF-Tg mice. As previously shown, dnNRSF-Tg hearts were highly susceptible to induction of VT (*Figure 3C*), whereas no induction of VT was detected in WT hearts, whether they were left untreated (*n* = 5) or treated with aliskiren

(*n* = 7). Furthermore, aliskiren strongly suppressed susceptibility of dnNRSF-Tg hearts to VTs, suggesting that aliskiren prevented the generation of arrhythmogenic re-entrant substrates (*Figure 3C*).

3.4 Deletion of AT1aR also prevents pathological cardiac remodelling and sudden death in dnNRSF-Tg mice

To further confirm that inhibition of RAS signalling is responsible for aliskiren-induced suppression of cardiac remodelling and sudden death in dnNRSF-Tg mice, we genetically deleted AT1aR from the mice by crossing dnNRSF-Tg mice with AT1aR knockout mice (AT1aR$^{-/-}$).[8] Heart-to-body weight ratios, which were significantly higher in dnNRSF-Tg;AT1aR$^{+/+}$ than in WT mice (*Figure 2A*), were significantly reduced in dnNRSF-Tg;AT1aR$^{-/-}$ mice (*Figure 3D* and *E*). Subsequent echocardiographic analysis revealed that LV diastolic dimension, LV systolic dimension, and ejection fraction were all significantly better in dnNRSF-Tg;AT1aR$^{-/-}$ than in dnNRSF-Tg;AT1aR$^{+/+}$ mice (*Figure 3F–H* and see Supplementary material online, *Table S1*). Ventricular expression of ANP, β-MHC, and skeletal α-actin mRNA, which were significantly higher in dnNRSF-Tg;AT1aR$^{+/+}$ than in WT mice (*Figure 2E–G*), were significantly lower in dnNRSF-Tg;AT1aR$^{-/-}$ than in dnNRSF-Tg;AT1aR$^{+/+}$ mice (*Figure 3I–K*). Conversely, levels of α-MHC and SERCA2 mRNA, which were reduced in dnNRSF-Tg;AT1aR$^{+/+}$ mice (*Figure 2H* and see Supplementary material online, *Figure S5A*), were significantly restored in dnNRSF-Tg;AT1aR$^{-/-}$ mice (*Figure 3L* and see Supplementary material online, *Figure S6A*). Mean myocyte size was also significantly reduced in dnNRSF-Tg;AT1aR$^{-/-}$ mice compared with dnNRSF-Tg;AT1aR$^{+/+}$ mice (see Supplementary material online, *Figure S6B*). Expression of ACE mRNA in dnNRSF-Tg;AT1aR$^{-/-}$ ventricles was significantly weaker than in dnNRSF-Tg;AT1aR$^{+/+}$ mice
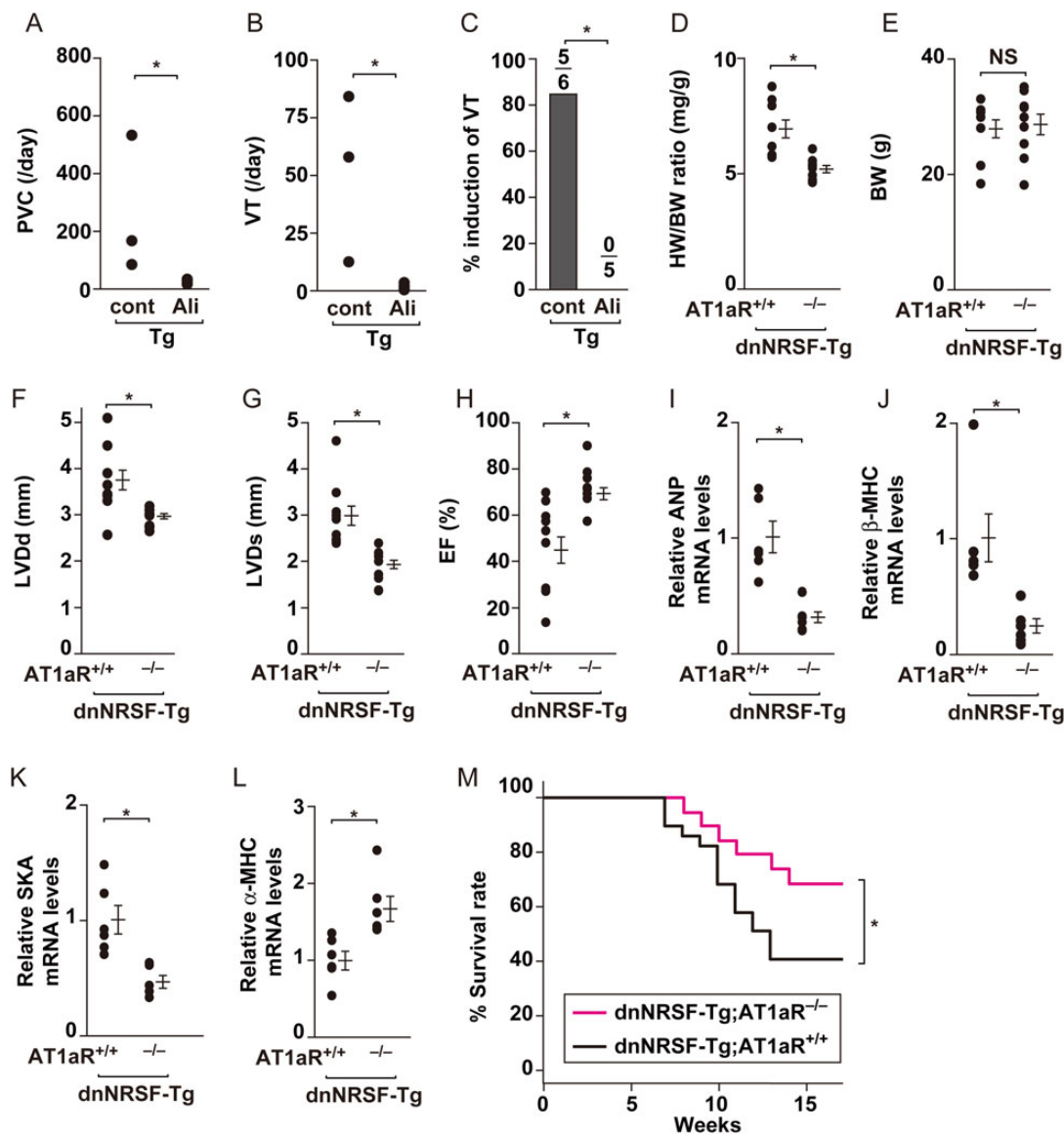
Figure 3 Effects of renin inhibition on arrhythmias and effects of genetic deletion of the AT1aR on cardiac remodelling and survival in dnNRSF-Tg mice. (A and B) Numbers of PVCs (A) and VTs (B) recorded using a telemetry system in 22-week-old dnNRSF-Tg, with or without 6 weeks of aliskiren treatment. Data are shown as dot plots. *$P < 0.05$ using the Mann−Whitney test ($n = 3$ for untreated Tg and 4 for Tg with aliskiren). (C) Incidence of VTs induced during intracardiac electrophysiology studies in 22-week-old Tg, with or without 6 weeks of aliskiren treatment. Upper numbers, numbers of mice with induced VT; lower numbers, total numbers of mice tested. *$P < 0.05$ using Fisher's exact test. (D and E) Heart weight-to-body weight ratios (HW/BW) (D) and body weights (BW) (E) in 18-week-old dnNRSF-Tg;AT1aR$^{+/+}$ and dnNRSF-Tg;AT1aR$^{-/-}$ mice ($n = 8$ for dnNRSF-Tg;AT1aR$^{+/+}$ and 9 for dnNRSF-Tg;AT1aR$^{-/-}$ mice). (F−H) Echocardiographic parameters in 16-week-old dnNRSF-Tg;AT1aR$^{+/+}$ and dnNRSF-Tg;AT1aR$^{-/-}$ mice. LV diastolic dimension (Dd; F), LV systolic dimension (Ds; G), and ejection fraction (EF; H) are shown ($n = 10$ each). (I−L) Relative levels of ANP (I), β-MHC (J), skeletal α-actin (SKA; K), and α-MHC (L) mRNA in hearts from 18-week-old dnNRSF-Tg;AT1aR$^{+/+}$ and dnNRSF-Tg;AT1aR$^{-/-}$ mice ($n = 6$ each). All data in D−L are shown as dot plots and means ± SEM. *$P < 0.05$. NS: not significant. (M) Kaplan−Meier survival curves for dnNRSF-Tg;AT1aR$^{+/+}$ and dnNRSF-Tg;AT1aR$^{-/-}$ ($n = 30$ for dnNRSF-Tg;AT1aR$^{+/+}$ and 20 for dnNRSF-Tg;AT1aR$^{-/-}$). *$P < 0.05$.

(see Supplementary material online, *Figure S6C*). Cardiac expression of AT1aR mRNA was undetectable in dnNRSF-Tg;AT1aR$^{-/-}$ mice (see Supplementary material online, *Figure S6D*). More importantly, dnNRSF-Tg;AT1aR$^{-/-}$ mice had better survival rates than dnNRSF-Tg; AT1aR$^{+/+}$ mice (*Figure 3M*). We previously reported no significant difference in cardiac structure, function, or arrhythmicity between AT1aR$^{-/-}$ mice and WT mice under basal conditions.[8]

3.5 Optical mapping reveals the arrhythmogenic mechanisms in dnNRSF-Tg hearts and the effects of renin inhibition on the electrophysiological properties

To investigate the electrophysiological mechanism underlying the occurrence of malignant arrhythmias in dnNRSF-Tg and the effect of
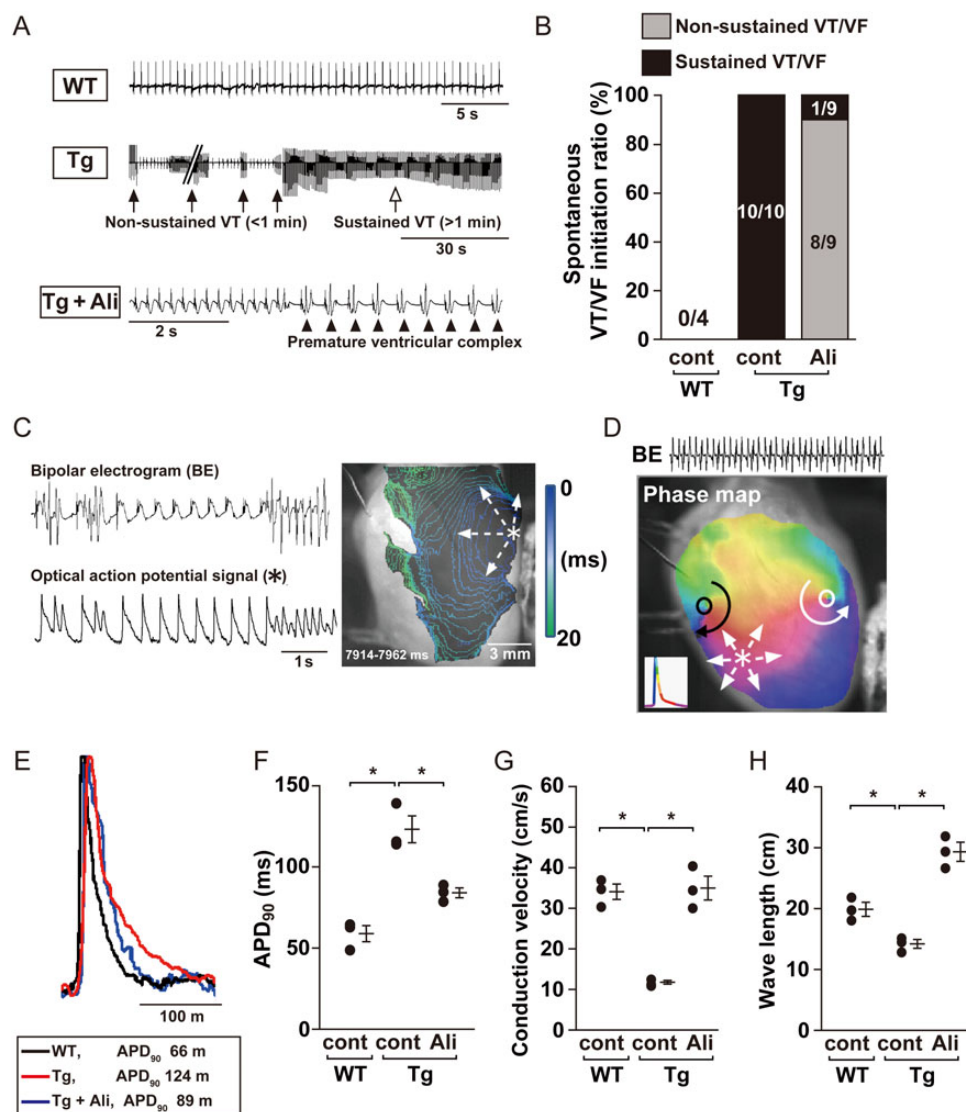
Figure 4 Optical mapping analysis of VT/VF in dnNRSF-Tg mice. (*A*) Representative bipolar electrocardiographs (ECG) from Langendorff-perfused hearts from WT, untreated dnNRSF-Tg (Tg), and dnNRSF-Tg treated for 6 weeks with aliskiren (Tg + Ali). The ECG from the untreated dnNRSF-Tg heart shows both repetitive non-sustained VT and sustained VT/VF, as indicated. The ECG from the aliskiren-treated dnNRSF-Tg heart shows a ventricular premature complex (ventricular bigeminy). (*B*) Incidence (%) of mice showing spontaneous sustained and non-sustained VT/VF in perfused hearts from WT (*n* = 4), Tg (*n* = 10), and Tg + Ali (*n* = 9). Mice used in the optical mapping experiments were 20−24 weeks of age. Black bars indicate the incidences of mice showing sustained VT/VF; grey bars indicate the incidences of mice showing non-sustained VT/VF without sustained VT/VF. The numbers of mice showing sustained VT/VF significantly differed between Tg and TG + Ali (*P* < 0.05 using Fisher's exact test). (*C*) Simultaneous recording of a bipolar ECG (left, top) and optical action potential signals (left, bottom) during the onset of non-sustained and sustained VTs in a perfused dnNRSF-Tg heart. The optical signals were recorded from the site indicated by the asterisk in the right panel. Right, isochrone activation map showing a breakthrough-type focal activation pattern during the onset of sustained VT. (*D*) Representative phase snap shot during a long-lasting VT episode in a dnNRSF-Tg heart. Complex interplay between figure-eight type re-entrant activity (circle and round arrows) and focal discharge (asterisk and arrows) was involved in the maintenance of arrhythmia. A bipolar ECG is shown above the image. (*E*) Superimposed representative optical action potential signals recorded from WT, Tg, and Tg + Ali hearts. The APD$_{90}$ (ms) for each action potential is indicated. (*F−H*) Graphs showing the APD$_{90}$ (*F*), conduction velocity (*G*), and wavelength (*H*) of the optical action potential signals in hearts of WT, Tg, and Tg + Ali (*n* = 3 each) during constant pacing (4 Hz). In (*F−H*), graphs are shown as dot plots and means ± SEM. *P < 0.05.

RAS inhibition on those arrhythmias, we used high-resolution epicardial optical mapping of membrane voltage to analyse action potential signals in Langendorff-perfused hearts from WT and dnNRSF-Tg.[9] In all of the hearts from untreated dnNRSF-Tg, we observed spontaneous sustained and non-sustained VT/VFs, whereas no VT/VFs were observed in control WT hearts (*Figure 4A* and *B*). Hearts from dnNRSF-Tg treated with aliskiren continued to show spontaneous PVCs and non-sustained VTs at a reduced frequency, but the incidence of sustained VT was markedly lower than in untreated dnNRSF-Tg hearts (*Figure 4A* and *B*). The epicardial activation pattern and optical action potential signals recorded from Langendorff-perfused ventricles of untreated dnNRSF-Tg revealed that VT/VFs were initiated following

breakthrough-type excitations, which originated from focal activation sites and then propagated over the entire ventricle (*Figure 4C* and see Supplementary material online, *Video S1*). Optical signals near the focal activation sites showed early afterdepolarization (EAD)-type triggered activity (*Figure 4C* and see Supplementary material online, *Video S1*). Furthermore, while breakthrough-type excitations were observed during the initial phase of VT/VFs, complex interplay between focal and re-entrant activity was involved in the maintenance of sustained VT/VFs in untreated dnNRSF-Tg hearts (*Figure 4D* and see Supplementary material online, *Video S2*). Under constant pacing, action potential duration (APD) was significantly prolonged and conduction velocity was markedly slower in untreated dnNRSF-Tg than WT (*Figure 4E–G* and see Supplementary material online, *Video S3*). Consequently, the wavelength was significantly shorter in untreated dnNRSF-Tg than WT, and favoured the formation and stability of functional re-entry (*Figure 4H*). In aliskiren-treated dnNRSF-Tg, the prolongation of APD was partially reversed and conduction velocity was completely restored, resulting in complete correction of the wavelength (*Figure 4E–H* and see Supplementary material online, *Video S3*), which could account for the dramatic reduction in the incidence of sustained VT (*Figures 3B* and *4B*).

3.6 Renin inhibition suppresses cardiac fibrosis and restores Cx43 expression in dnNRSF-Tg ventricles

To begin to determine the molecular mechanism responsible for the conduction delay and the generation of arrhythmogenic substrates in dnNRSF-Tg and its reversal by aliskiren, we examined the contribution of cardiac fibrosis, which is known to slow conduction and create a substrate vulnerable to re-entry.[3,11] Masson's trichrome staining revealed that interstitial fibrosis in dnNRSF-Tg was significantly diminished by aliskiren (*Figure 5A* and *B*). Consistent with that finding, the expression of fibrosis-related genes, including transforming growth factor-β1 (TGFβ-1), TGFβ-3, collagen type 1 α1, fibronectin, tissue inhibitor of metalloproteinase (TIMP)-1, and MMP-2, was significantly elevated in untreated dnNRSF-Tg (*Figure 5C–H*), and the TIMP-1/MMP2 ratio was significantly increased (*Figure 5I*). These increases were almost completely blocked in dnNRSF-Tg mice treated with aliskiren (*Figure 5C–I*). Furthermore, the increase in interstitial fibrosis seen in dnNRSF-Tg ventricles was significantly suppressed in dnNRSF-Tg;AT1aR$^{-/-}$ ventricles (see Supplementary material online, *Figure S6E*). In addition, the expression of TGFβ-1, TGFβ-3, collagen type 1 α1, fibronectin, TIMP-1, and MMP-2 mRNA as well as the TIMP-1/MMP2 ratio were all significantly reduced in dnNRSF-Tg;AT1aR$^{-/-}$ ventricles, when compared with dnNRSF-Tg;AT1aR$^{+/+}$ ventricles (see Supplementary material online, *Figure S6F–L*).

We also focused on the expression of Cx43, which is the principle component of gap junctions in the adult cardiac ventricle.[12] Cx43 deficiency reportedly leads to a slowing of conduction velocity and to ventricular arrhythmias.[13] Immunohistochemical labelling showed that Cx43 expression, measured as the Cx43-positive area, was significantly weaker in untreated dnNRSF-Tg than in WT ventricles, and that aliskiren restored Cx43 expression in dnNRSF-Tg hearts (*Figure 6A* and *B*). We observed that in WT ventricles, Cx43 is expressed almost entirely in troponin T-positive cardiac myocytes, and that in aliskiren-treated dnNRSF-Tg ventricles, Cx43 expression is restored to troponin T-positive cardiac myocytes (see Supplementary material online, *Figure S7A*). Consistent with that finding, western blot analysis showed

that Cx43 levels are significantly lower in untreated dnNRSF-Tg than in untreated WT ventricles, but that aliskiren restored Cx43 expression in dnNRSF-Tg ventricles (*Figure 6C* and *D*). Levels of Cx43 mRNA did not significantly differ among untreated WT, untreated dnNRSF-Tg, and aliskiren-treated dnNRSF-Tg hearts, suggesting that the altered Cx43 levels reflect post-translational regulation (see Supplementary material online, *Figure S7B*). In WT mice, aliskiren treatment did not significantly affect levels of Cx43 protein (see Supplementary material online, *Figure S7C* and *D*). Similar restoration of Cx43 was observed in dnNRSF-Tg;AT1aR$^{-/-}$ ventricles (see Supplementary material online, *Figure S7E*). It is known that Cx43 levels and its function are regulated by phosphorylation by several kinases.[14] For example, phosphorylation of two serine residues, Ser279/282, by p42/44 MAPK leads to a reduction in gap junction communication and initiates Cx43 turnover.[14] When we examined the phosphorylation status of Cx43 in WT and dnNRSF-Tg ventricles using several phospho-specific antibodies, we found that the level of Cx43 Ser279/282 phosphorylation was higher in untreated dnNRSF-Tg than in untreated WT ventricles, and that the levels in dnNRSF-Tg ventricles were significantly reduced by aliskiren (*Figure 6E* and *F*). In WT mice, aliskiren treatment did not significantly affect Cx43 Ser279/282 phosphorylation (see Supplementary material online, *Figure S7C* and *F*). Consistent with the increased Cx43 Ser279/282 phosphorylation, levels of both activated and total p42/44 MAPK were higher in untreated dnNRSF-Tg than in untreated WT ventricles, but they were reduced by aliskiren treatment in dnNRSF-Tg ventricles (*Figure 6E*). The relative levels of activated (phosphorylated) p42/44 MAPK normalized to total p42/44 MAPK were also higher in untreated dnNRSF-Tg than in untreated WT ventricles, but they too were reduced by aliskiren treatment in dnNRSF-Tg ventricles (see Supplementary material online, *Figure S7G*). In WT mice, aliskiren treatment did not significantly affect either activated or total p42/44 MAPK levels (see Supplementary material online, *Figure S7C* and *H*). These results demonstrate that cardiac fibrosis and reduced expression of Cx43, at least in part, contribute to the conduction delay in dnNRSF-Tg ventricles, and that preventing these events is associated with restoration of the conduction velocity.

4. Discussion

In the present study, we demonstrated that pharmacological blockade of RAS signalling using the renin inhibitor aliskiren significantly reduced pathological cardiac remodelling and the resultant increase in the incidences of malignant arrhythmias and sudden death in dnNRSF-Tg mice, a mouse model of non-ischaemic cardiomyopathy with lethal arrhythmias.[4] The mode of death in dnNRSF-Tg mice is sudden and without overt oedema, pleural effusion or apparent lung congestion, and all of the telemetry data obtained at the time of death indicates VT/VF to be the cause.[4] Optical mapping of cardiac action potentials revealed that EAD-type triggered activity induced by excessive APD prolongation and functional re-entry associated with decreased conduction velocity contribute to the initiation and maintenance of VT/VF in failing hearts in dnNRSF-Tg. Aliskiren treatment significantly reversed the slowed conduction velocity, thereby disrupting the maintenance of re-entry. Prevention of the decline in Cx43 expression and the suppression of interstitial fibrosis presumably mediated the observed aliskiren-induced reduction of arrhythmogenicity, at least in part. Genetic deletion of AT1aR in dnNRSF-Tg similarly ameliorated pathological LV remodelling and prolonged the survival. Collectively, these results clearly indicate that by increasing interstitial
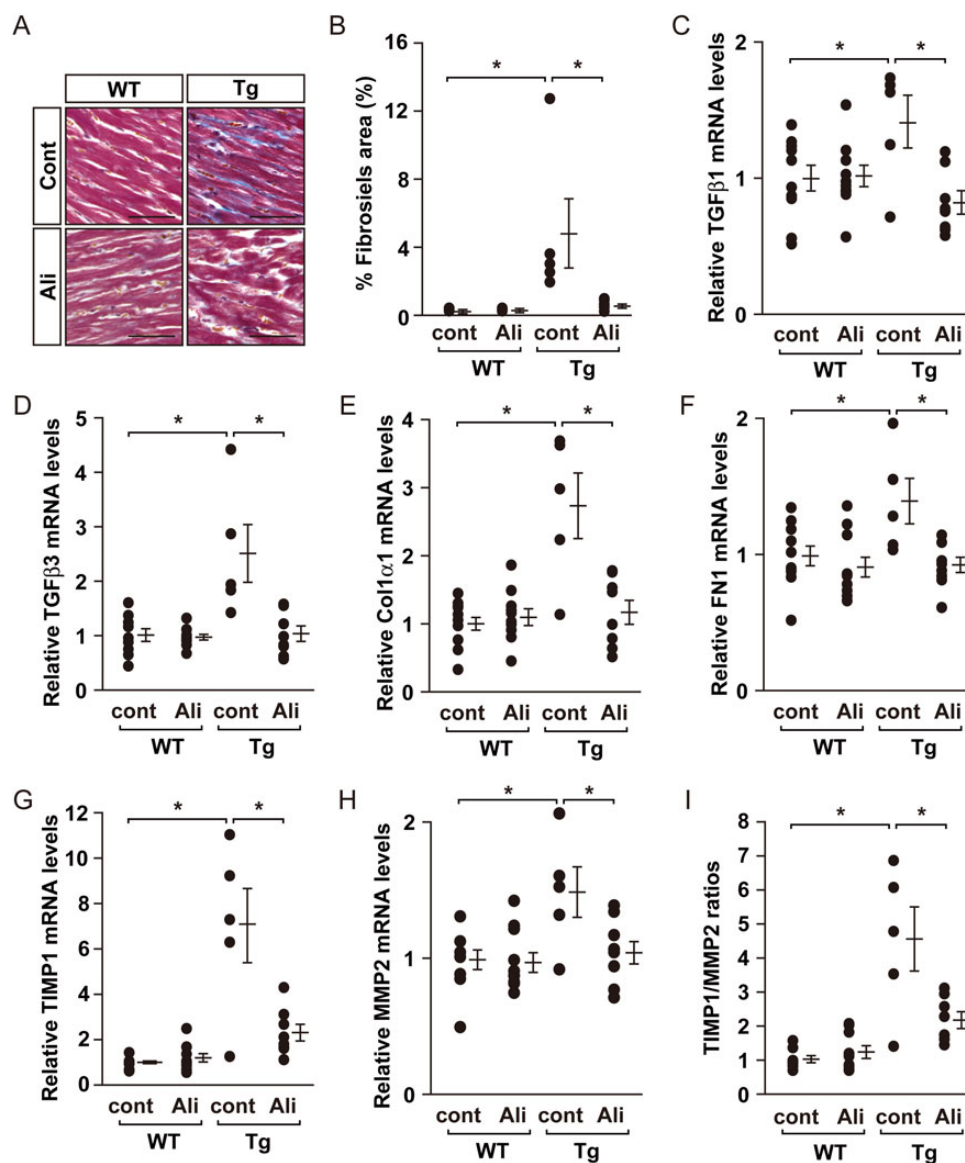
Figure 5 Renin inhibition suppresses cardiac fibrosis in dnNRSF-Tg mice. (A) Histological analysis of hearts from WT and dnNRSF-Tg, with or without aliskiren. Shown are photomicrographs of Masson's trichrome-stained sections of the left ventricle. Scale bars, 50 μm. (B) Graphs showing the % collagen area in hearts from WT and dnNRSF-Tg, with or without aliskiren ($n = 6$ for untreated WT, 7 for WT with aliskiren, 5 for untreated Tg, and 8 for Tg with aliskiren). (C−H) Relative levels of TGFβ-1 (C), TGFβ-3 (D), collagen type 1 α1 (Col1α1; E), fibronectin (FN1; F), TIMP1 (G), and MMP-2 (H) mRNA in hearts from WT and dnNRSF-Tg, with or without aliskiren. (I) TIMP-1/MMP2 ratios in hearts from WT and dnNRSF-Tg, with or without aliskiren. In all graphs, $n = 10$ for untreated WT and WT with aliskiren, 5 for untreated Tg, and $n = 8$ for Tg with aliskiren. Aliskiren treatment began when the mice were 16 weeks of age and lasted 12 weeks. All data are shown as dot plots and means $\pm$ SEM. *$P < 0.05$.

fibrosis and reducing expression of Cx43, RAS signalling acts as a key promoter of remodelling that leads to the generation of arrhythmogenic substrates in failing hearts, and thus contributes to the occurrence of lethal arrhythmias.

We previously showed that expression of fetal cardiac ion channels (i.e. TCCs and HCN channels) is significantly increased in dnNRSF-Tg ventricles, and that inhibition of these channels improves survival by reducing the incidence of malignant arrhythmias without ameliorating cardiac remodelling.[5,6] This suggests that these channels do not predominantly contribute to the pathological cardiac remodelling seen in this mouse model, but are instead involved in the triggering of

arrhythmias, i.e. the increased triggering of arrhythmias reflects ion channel alterations initiated by the genetic inhibition of NRSF. In contrast, aliskiren significantly ameliorated pathological cardiac remodelling in dnNRSF-Tg mice, which in turn reduced the incidences of malignant arrhythmias and sudden death. Optical mapping analysis revealed that aliskiren improved conduction velocity and strongly suppressed the incidence of sustained VT in dnNRSF-Tg hearts. Taken together with the results of our earlier studies, these findings suggest that the increased triggering of arrhythmias reflects ion channel alterations initiated by the genetic inhibition of NRSF. Moreover, the progression of arrhythmogenic substrates, which is mediated by RAS
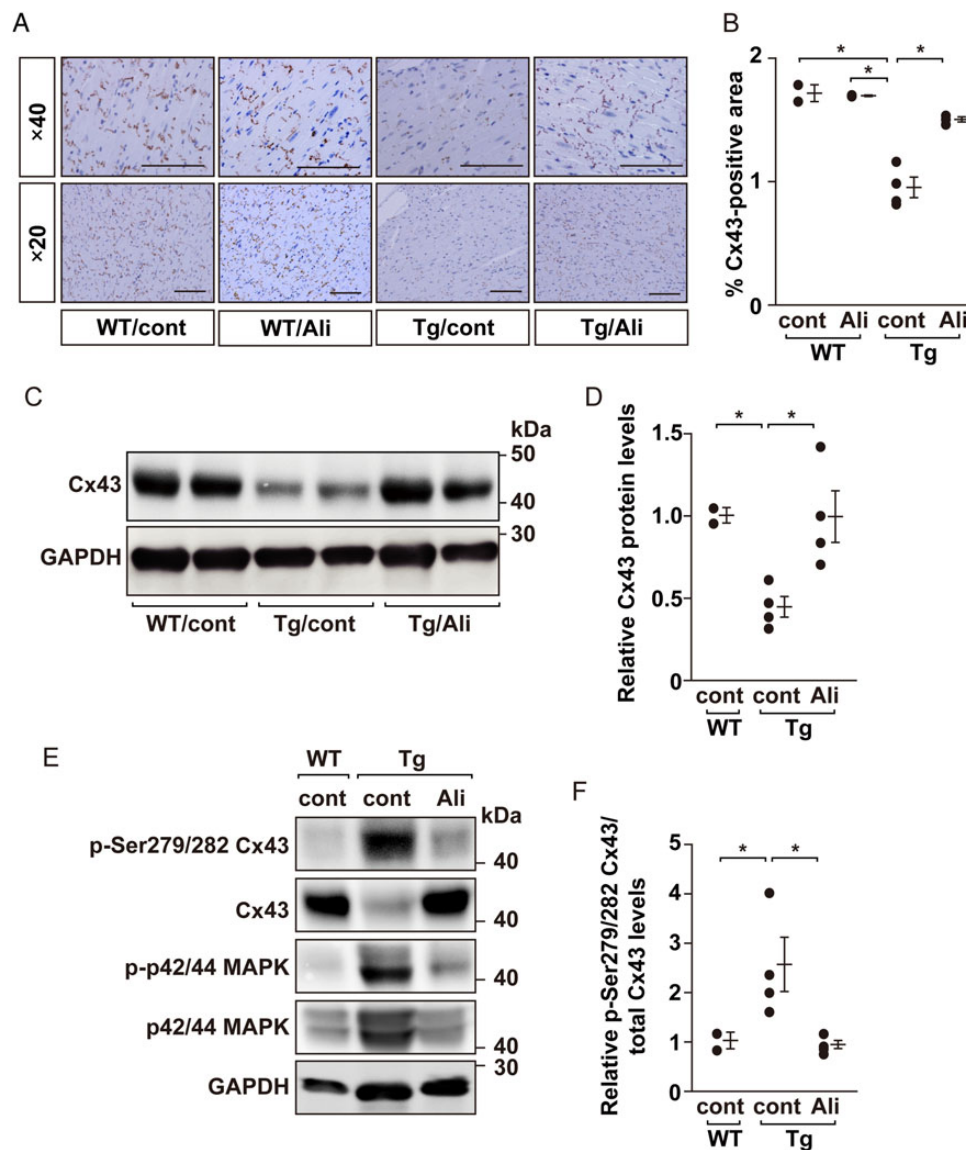
Figure 6 Renin inhibition prevents the reduction in Cx43 expression in dnNRSF-Tg hearts. (A) Immunostaining of Cx43 in hearts from WT and dnNRSF-Tg, with or without aliskiren treatment. Scale bars: 100 μm. (B) Graph showing the levels of Cx43 expression measured as Cx43-positive area ($n = 2$ for untreated WT and aliskiren-treated WT, 4 for untreated Tg, and 3 for aliskiren-treated Tg mice). (C) Western blot analysis of Cx43 and GAPDH expression in the ventricles from WT and dnNRSF-Tg, with or without aliskiren treatment. (D) Relative Cx43 levels in the ventricles of WT ($n = 2$) and dnNRSF-Tg, with ($n = 4$) or without aliskiren ($n = 4$). Cx43 levels were normalized to those of GAPDH. The relative Cx43 level in untreated WT mice was assigned a value of 1.0. (E) Representative western blot analysis of Ser279/282-phosphorylated Cx43, unphosphorylated Cx43, phosphorylated p42/44 MAPK, total p42/44 MAPK, and GAPDH in the ventricles of WT and dnNRSF-Tg, with or without aliskiren. (F) Relative Ser279/282-phosphorylated Cx43 levels normalized to the total Cx43 in ventricles from WT ($n = 2$) and dnNRSF-Tg, with ($n = 4$) or without aliskiren ($n = 4$). Aliskiren treatment began when the mice were 16 weeks of age and lasted 12 weeks. All data are shown as dot plots and means ± SEM. *$P < 0.05$.

activation, contributes synergistically to the occurrence of malignant arrhythmias and sudden cardiac death in dnNRSF-Tg mice.[5,6]

A link between RAS signalling, altered Cx43 regulation, and increased arrhythmicity has been suggested in several studies.[8,15,16] However, that link had never been evaluated in a model of heart failure showing spontaneous malignant arrhythmias and sudden cardiac death, and the underlying electrophysiological mechanisms remained unreported. By using dnNRSF-Tg mice, we were able to reveal the critical contribution made by the RAS to the generation of malignant arrhythmias and the underlying arrhythmogenic mechanisms, which involve the dysregulation of Cx43 and increased cardiac fibrosis, both of which contribute to a reduction in conduction velocity.

Renin was recently reported to affect cardiovascular function and remodelling through the (pro) renin receptor independently of the generation of angiotensin II.[17] It may be that the effects of the renin inhibitor aliskiren observed in the present study are mediated in part via this alternative pathway. However, it is unlikely that pathway is a major contributor to the observed effect of aliskiren in this study, as deletion of AT1aR from dnNRSF-Tg mice produced phenotypes similar to aliskiren treatment. Given the differences in the experimental conditions

used for pharmacological inhibition with aliskiren and genetic deletion of AT1aR, it is difficult to precisely address the differential contributions made by renin and angiotensin II to cardiac remodelling in this study. Aldosterone, downstream of RAS, is also involved in pathological cardiac remodelling. Indeed, in several clinical trials, administration of a mineral corticoid receptor antagonist suppressed sudden cardiac death in patients with heart failure.[18] In the present study, aliskiren suppressed plasma aldosterone in dnNRSF-Tg mice nearly to the levels seen in control WT mice. Elucidation of the precise roles played by each component of the RAS could potentially serve as the basis for the development of a more effective strategy to prevent sudden cardiac death in heart failure. In that context, NRSF reportedly regulate aldosterone synthase (CYP11B2) and 11β-hydroxylase (CYP11B1) gene expression in adrenal cells.[19] As cardiac expression of these genes is very weak and does not significantly differ between dnNRSF-Tg and WT ventricles (unpublished observations), we think it is unlikely that elevated cardiac aldosterone synthase directly induced by NRSF inhibition is responsible for the increased plasma aldosterone levels seen in dnNRSF-Tg mice.

In the ASTRONAUT trial, the effect of aliskiren on post-discharge outcomes among patients hospitalized for heart failure was tested by adding the drug to the standard therapy, which included ACE inhibitors or angiotensin receptor blockers and β-blockers.[20] Under those conditions, aliskiren showed no significant effect on primary endpoints. In our study, aliskiren was administered to untreated mice with cardiac dysfunction. Furthermore, a recent subgroup analysis of the ASTRONAUT trial showed that adding aliskiren to the standard therapy improves post-discharge outcomes in non-diabetic patients hospitalized for heart failure.[21] Future investigation is needed to confirm the potential benefits of renin inhibition under these conditions.

In this study, we did not assess the sodium current (I_{Na}), which is also an important determinant of conduction velocity in ventricular myocardium,[3] because the amplitude of I_{Na} is too large to correctly measure under physiological conditions in isolated myocytes. The role of changes in I_{Na} in the failing hearts is somewhat controversial, however.[3] Nevertheless, as the resting membrane potentials in ventricular myocytes from dnNRSF-Tg are more depolarized than those from WT,[5] there is a possibility that reduced availability of I_{Na} is also involved in the conduction delay observed in the dnNRSF-Tg ventricular myocardium. In addition, we did not perform a detailed analysis of the effects of RAS blockade on cardiac myocyte kinetics and mechanics in isolated cells; we used echocardiography and LV catheterization to evaluate cardiac systolic and diastolic function *in vivo*. Furthermore, because it is impossible to completely rule out that some dnNRSF-Tg mice (especially older mice) died due to congestive heart failure, despite the arrhythmias, there is still a possibility that RAS inhibition may also prevent this mode of death, in addition to sudden arrhythmic death, in dnNRSF-Tg mice. We anticipate that further investigation will lead to the development of more effective pharmacological approaches to preventing lethal arrhythmias in patients with heart failure.

Supplementary material

Supplementary material is available at *Cardiovascular Research* online.

Acknowledgements

We thank Yukari Kubo for her excellent secretarial work and Miku Ohya, Akiko Abe, and Mizuho Takemura for their excellent technical support.

References

1. Tomaselli GF, Marban E. Electrophysiological remodeling in hypertrophy and heart failure. *Cardiovasc Res* 1999;**42**:270–283.
2. Boukens BJ, Christoffels VM, Coronel R, Moorman AF. Developmental basis for electrophysiological heterogeneity in the ventricular and outflow tract myocardium as a substrate for life-threatening ventricular arrhythmias. *Circ Res* 2009;**104**:19–31.
3. Tomaselli GF, Zipes DP. What causes sudden death in heart failure? *Circ Res* 2004;**95**: 754–763.
4. Kuwahara K, Saito Y, Takano M, Arai Y, Yasuno S, Nakagawa Y, Takahashi N, Adachi Y, Takemura G, Horie M, Miyamoto Y, Morisaki T, Kuratomi S, Noma A, Fujiwara H, Yoshimasa Y, Kinoshita H, Kawakami R, Kishimoto I, Nakanishi M, Usami S, Saito Y, Harada M, Nakao K. NRSF regulates the fetal cardiac gene program and maintains normal cardiac structure and function. *EMBO J* 2003;**22**:6310–6321.
5. Kinoshita H, Kuwahara K, Takano M, Arai Y, Kuwabara Y, Yasuno S, Nakagawa Y, Nakanishi M, Harada M, Fujiwara M, Murakami M, Ueshima K, Nakao K. T-type Ca^{2+} channel blockade prevents sudden death in mice with heart failure. *Circulation* 2009; **120**:743–752.
6. Kuwabara Y, Kuwahara K, Takano M, Kinoshita H, Arai Y, Yasuno S, Nakagawa Y, Igata S, Usami S, Minami T, Yamada Y, Nakao K, Yamada C, Shibata J, Nishikimi T, Ueshima K, Nakao K. Increased expression of HCN channels in the ventricular myocardium contributes to enhanced arrhythmicity in mouse failing hearts. *J Am Heart Assoc* 2013;**2**: e000150.
7. Lu H, Rateri DL, Feldman RJ Jr, Fukamizu A, Ishida J, Oesterling EG, Cassis LA, Daugherty A. Renin inhibition reduces hypercholesterolemia-induced atherosclerosis in mice. *J Clin Invest* 2008;**118**:984–993.
8. Yasuno S, Kuwahara K, Kinoshita H, Yamada C, Nakagawa Y, Usami S, Kuwabara Y, Ueshima K, Harada M, Nishikimi T, Nakao K. Angiotensin II type 1a receptor signalling directly contributes to the increased arrhythmogenicity in cardiac hypertrophy. *Br J Pharmacol* 2013;**170**:1384–1395.
9. Yamazaki M, Honjo H, Nakagawa H, Ishiguro YS, Okuno Y, Amino M, Sakuma I, Kamiya K, Kodama I. Mechanisms of destabilization and early termination of spiral wave reentry in the ventricle by a class III antiarrhythmic agent, nifekalant. *Am J Physiol Heart Circ Physiol* 2007;**292**:H539–H548.
10. Gao S, Ho D, Vatner DE, Vatner SF. Echocardiography in mice. *Curr Protoc Mouse Biol* 2011;**1**:71–83.
11. Nguyen TP, Qu Z, Weiss JN. Cardiac fibrosis and arrhythmogenesis: the road to repair is paved with perils. *J Mol Cell Cardiol* 2014;**70**:83–91.
12. Akar FG, Spragg DD, Tunin RS, Kass DA, Tomaselli GF. Mechanisms underlying conduction slowing and arrhythmogenesis in nonischemic dilated cardiomyopathy. *Circ Res* 2004;**95**:717–725.
13. Gutstein DE, Morley GE, Tamaddon H, Vaidya D, Schneider MD, Chen J, Chien KR, Stuhlmann H, Fishman GI. Conduction slowing and sudden arrhythmic death in mice with cardiac-restricted inactivation of connexin 43. *Circ Res* 2001;**88**:333–339.
14. Solan JL, Lampe PD. Specific Cx43 phosphorylation events regulate gap junction turnover in vivo. *FEBS Lett* 2014;**588**:1423–1429.
15. Sovari AA, Iravanian S, Dolmatova E, Jiao Z, Liu H, Zandieh S, Kumar V, Wang K, Bernstein KE, Bonini MG, Duffy HS, Dudley SC. Inhibition of c-Src tyrosine kinase prevents angiotensin II-mediated connexin-43 remodeling and sudden cardiac death. *J Am Coll Cardiol* 2011;**58**:2332–2339.
16. Yoshida M, Ohkusa T, Nakashima T, Takanari H, Yano M, Takemura G, Honjo H, Kodama I, Mizukami Y, Matsuzaki M. Alterations in adhesion junction precede gap junction remodelling during the development of heart failure in cardiomyopathic hamsters. *Cardiovasc Res* 2011;**92**:95–105.
17. Nguyen G, Danser AH. Prorenin and (pro)renin receptor: a review of available data from in vitro studies and experimental models in rodents. *Exp Physiol* 2008;**93**: 557–563.
18. Al Chekakie MO. Traditional heart failure medications and sudden cardiac death prevention: a review. *J Cardiovasc Pharmacol Ther* 2013;**18**:412–426.
19. Somekawa S, Imagawa K, Naya N, Takemoto Y, Onoue K, Okayama S, Takeda Y, Kawata H, Horii M, Nakajima T, Uemura S, Mochizuki N, Saito Y. Regulation of aldosterone and cortisol production by the transcriptional repressor neuron restrictive silencer factor. *Endocrinology* 2009;**150**:3110–3117.

20. Gheorghiade M, Bohm M, Greene SJ, Fonarow GC, Lewis EF, Zannad F, Solomon SD, Baschiera F, Botha J, Hua TA, Gimpelewicz CR, Jaumont X, Lesogor A, Maggioni AP, Investigators ASTRONAUT, Coordinators. Effect of aliskiren on postdischarge mortality and heart failure readmissions among patients hospitalized for heart failure: the ASTRONAUT randomized trial. *JAMA* 2013;**309**:1125−1135.

21. Maggioni AP, Greene SJ, Fonarow GC, Bohm M, Zannad F, Solomon SD, Lewis EF, Baschiera F, Hua TA, Gimpelewicz CR, Lesogor A, Gheorghiade M, Investigators ASTRONAUT, Coordinators. Effect of aliskiren on post-discharge outcomes among diabetic and non-diabetic patients hospitalized for heart failure: insights from the ASTRONAUT trial. *Eur Heart J* 2013;**34**:3117−3127.